Phosphides-based terahertz quantum-cascade laser

*D. V. Ushakov[1], A. A. Afonenko[1], R. A. Khabibullin,[2,3] M. A. Fadeev[4], and A. A. Dubinov[4,5,]**

[1]Belarusian State University, 4 Nezavisimosti Avenue, Minsk, 220030, Belarus
[2]V.G. Mokerov Institute of Ultra-High Frequency Semiconductor Electronics RAS, 7/5 Nagornyy Proezd, Moscow, 117105, Russia
[3]Moscow Institute of Physics and Technology, 9 Institutsky Lane, Dolgoprudny, 141701, Russia
[4]Institute for Physics of Microstructures, Russian Academy of Sciences, GSP-105, Nizhny Novgorod, 603950, Russia
[5]Lobachevsky State University of Nizhny Novgorod, 23 Gagarina Avenue, Nizhny Novgorod, 603950, Russia
*E-mail: sanya@ipmras.ru

Keywords: quantum cascade laser, terahertz, phosphides, GaAs phonon absorption band region

Abstract

Due to their high optical phonon energies GaInP/AlGaInP heterostructures are a promising active medium to solve the problem of creating compact semiconductor sources with an operating frequency range of 5.5-7 THz. In this work, the temperature dependences of gain and absorption at 6.4-6.9 THz have been calculated for a GaInP/AlGaInP-based quantum-cascade laser (QCL) with two quantum wells in the cascade and a metal-metal waveguide. The dielectric function and mode losses for a 10 μm thick Au-Au waveguide, based on ternary InGaP and quaternary AlGaInP semiconductors, have been investigated in details. We propose a laser structure that provides a mode gain of over 100 cm^{-1} with a maximum operating temperature about 100 K. The results of this study open the way to the development of a QCL for operation in a significant part of the GaAs phonon absorption band region, which is inaccessible for existing QCLs.

1. Introduction

Since their invention two decades ago THz quantum cascade lasers (QCLs) have progressed from cryogenic devices with relatively small output power [1] to powerful THz sources

operating under thermoelectric Peltier cooling.[2, 3] However, QCLs are not yet available in the range from 5.5 to 10.5 THz despite its importance in such applications as spectroscopy of organic and non-organic materials, liquids and gases.[4-7] The main obstacle for making QCLs for this range is a strong phonon absorption in the materials that they are made of (GaAs/AlGaAs, InGaAs/InAlAs).[8, 9] Therefore, semiconductors with a different energy of polar-optical phonons can serve as an alternative to group III metal arsenides for the creation of QCLs. Previously, both $A_{III}B_V$ materials (GaN/AlGaN [10]) and $A_{II}B_{VI}$ materials (ZnO/MgZnO [11], ZnSe/ZnMgSe [12], HgCdTe [13]) were suggested as such semiconductors. It has also been suggested using van der Waals heterostructures of 2D - materials with graphene.[14] However, the experimental realization of QCLs based on the proposed materials showed only spontaneous electroluminescence due to the complexity of precise growth of hundreds of nanoscale layers of these materials (see, for example, works on GaN/AlGaN [15], ZnO/MgZnO [16]) or difficulty to form ideal structures based on 2D materials.[17] Note also that due to the strong two-phonon absorption in the HgCdTe, lasing in it at intersubband transitions at frequencies below 7 THz is unlikely.[18]

In this paper we investigate the prospects of using a material system based on group III metal phosphides (GaInP/AlGaInP) for creating a double metal waveguide QCL with generation frequency of ~ 7 THz. The choice of this heteropair is explained by the fact that GaInP and AlGaInP are polar semiconductors with optical phonon frequencies in the range of 10–12 THz, which is higher than that of the traditional GaAs/AlGaAs heteropair (phonon energy ~ 8 THz).[19] A major advantage of phosphide-based heterostructures is the developed growth technology using both molecular beam epitaxy and vapor deposition. Similarly to GaAs, GaInP and AlGaInP have a zinc blende lattice structure. The lattice constants of $Ga_{0.51}In_{0.49}P/(Al_xGa_{1-x})_{0.51}In_{0.49}P/GaAs$ are very close, which allows the growth of relaxed multilayer structures on GaAs substrates. In addition, quite a lot of work has been devoted to the growth of high-quality GaInP/AlGaInP superlattices with thickness up to 1.8 μm, which were used to create red-orange interband lasers (see, for example, Ref. [20-25]).

2. Structures design and modeling

To model the THz QCL based on GaInP/AlGaInP, we used a model based on a system of balance equations for localized states and continuum states. To account for the effects of dephasing on the charge transport processes, we employed the technique of modifying the eigenbasis of Schrödinger equation by reducing the dipole moments of tunnel-bound states. The algorithm for calculating optoelectronic properties includes determining the energy levels and

wave functions based on the solution of Schrödinger equation within 3-band **k·p**-approximation, calculating matrix elements of dipole transitions, calculating scattering rates on optical phonons [26, 27], ionized impurities[26], roughness of hetero-boundaries [28, 29] and an electron-electron scattering[27], determining surface concentrations of carriers for the corresponding energy subbands from the closed system of balance equations, calculating the electric current and amplification spectra. The details of the calculation method tested on GaAs/AlGaAs heterostructure and a comparison of the calculations with experimental results showing good agreement can be found in Ref. [30, 31].

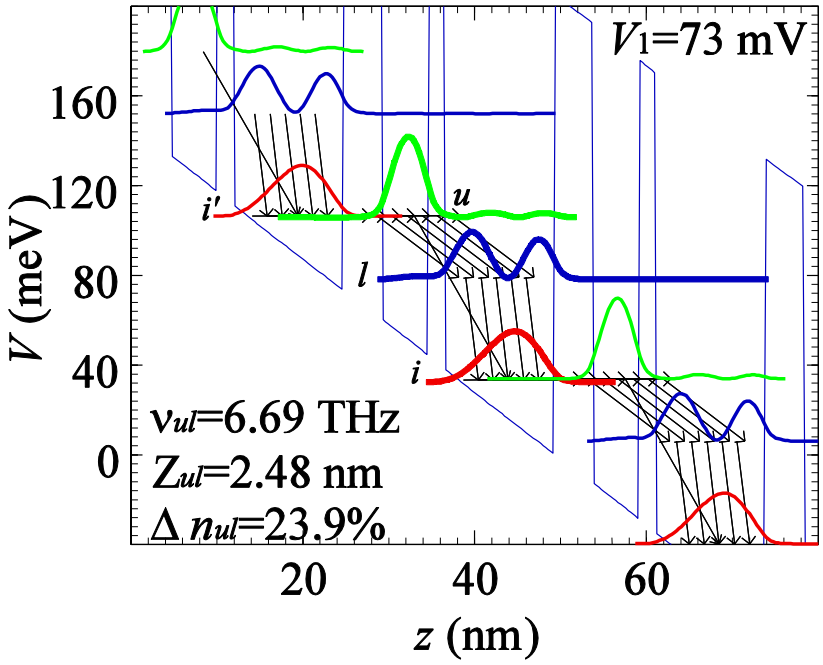

Figure 1. Energy profile of the bottom of the conduction band *V*, energy levels and squares of the moduli of the wave functions in the growth direction of the proposed structure at the value of the applied voltage V_1 = 73 mV per cascade and temperature T = 77 K. The number of arrows is proportional to the current density.

For our calculations we chose with the design with two quantum wells (QWs) in a cascade and a resonant-phonon depopulation scheme, when the operating voltage multiplied by the electron charge q in one cascade is close to the sum of the energies of the radiated photon and the longitudinal optical phonon. Our choice of the number of QWs in a cascade is justified by the operating temperatures of THz QCLs based on GaAs/AlGaAs with two-QW design being the highest.[3] In the course of optimization (scanning the thicknesses of the layers of the structure to obtain the highest gain at ~6.7 THz), we found the following sequence of layers in one cascade in nm: **4.52**/5.36/**1.98**/12.7 (**16**/19/**7**/45 monolayers of the corresponding semiconductor) with $(Al_{0.5}Ga_{0.5})_{0.51}In_{0.49}P$ barriers (in bold) and $Ga_{0.51}In_{0.49}P$ QWs (see Fig. 1).

The underlined QW is assumed to be doped with a layer electron concentration of 4.64×10^{10} cm^{-2}.

At the operation bias point V_1= 73 mV per cascade, injector level (*i*') and upper laser level (*u*) are aligned which leads to the resonant tunneling of electrons. The transition of an electron from the upper laser level (*u*) to the lower laser levels (*l*) is accompanied by the diagonal THz photon emission (ν_{ul} = 6.7 THz) with dipole matrix element Z_{ul} = 2.5 nm and high population inversion of approximately ~24%. Finally, electrons in the lower lasing levels relax to the injector level (*i*) through fast electron–longitudinal phonon scattering. This process then repeats in the subsequent cascades.

The scattering rates were calculated in the random-phase approximation with averaging of matrix elements over the electronic states in the subbands for a non-degenerate electron gas in the thermodynamic equilibrium conditions. Alloy-disorder scattering might play a significant role for a disordered quaternary alloy. The mathematical description of alloy-disorder scattering is based on the correlation function of fluctuations, just like the scattering by interface roughness. Since we were unable to find quantitative characteristics of this scattering mechanism, and expecting that scattering in GaInP/AlGaInP superlattices will be greater than in GaAs/AlGaAs and InGaAs/InAlAs structures, we used an increased effective roughness of 0.31 nm and correlation length of 9 nm compared to 0.1 nm and 6 nm in GaAs/AlGaAs and InGaAs/InAlAs structures [28, 29]. Thus, the roughness scattering rate in the calculations was about 20 times higher than for traditional heterostructures.

Table 1. Energies (*E*), relative level populations (N_{2D}), and scattering parameters for various mechanisms at V_1 = 73 mV.

#	N_{2D}	*E*, meV	γ_{tun}, meV	γ_{ph}, meV	γ_{ee}, meV	γ_{imp}, meV	γ_{rough}, meV	γ_{tot}, meV
i'	0.59	0.00	0.27	0.00080	0.0060	0.072	0.0080	0.36
u	0.32	0.43	0.29	0.059	0.035	0.12	0.17	0.66
l	0.082	-27.25	0.0014	0.70	0.011	0.099	0.091	0.90

The broadening parameter for the selected level *j* includes the components of scattering by tunneling (γ_{tun}), scattering by optical phonons (γ_{phon}), impurities (γ_{imp}), heterointerface roughness (γ_{rough}) and electron-electron scattering (γ_{ee}): $\gamma_{tot} = \gamma_{tun} + \gamma_{ph} + \gamma_{imp} + \gamma_{rough} + \gamma_{ee}$. As it can be seen from Table 1, in the proposed design, roughness scattering is not the dominant mechanism for level broadening. Transitions from the injector to the upper laser level (probability 1.1×10^{12} s^{-1}) are caused mainly by tunneling, and depletion of the lower laser level (probability 2.5×10^{12} s^{-1}) is ensured by resonant emission of phonons. The roughness and alloy-

disorder scattering mainly determine the rate of non-radiative transitions from the upper laser level to the lower one (73% of the total probability 6.6×10^{11} s^{-1}). Calculations show that laser generation in the proposed structure is maintained at 77 K with the effective roughness up to 0.37 nm.

The gain in the design under consideration occurs on the positive branch of the current-voltage characteristic up to ~76 mV, which is necessary to fulfill the condition of electrical stability at the operating point (Fig. 2). The lasing is achieved at voltages of ~68–76 mV. The current-voltage characteristic has an additional "parasitic" peak at a voltage below the lasing threshold in the region of 43 mV, which is associated with resonant tunneling of electrons between the injector and extractor levels.

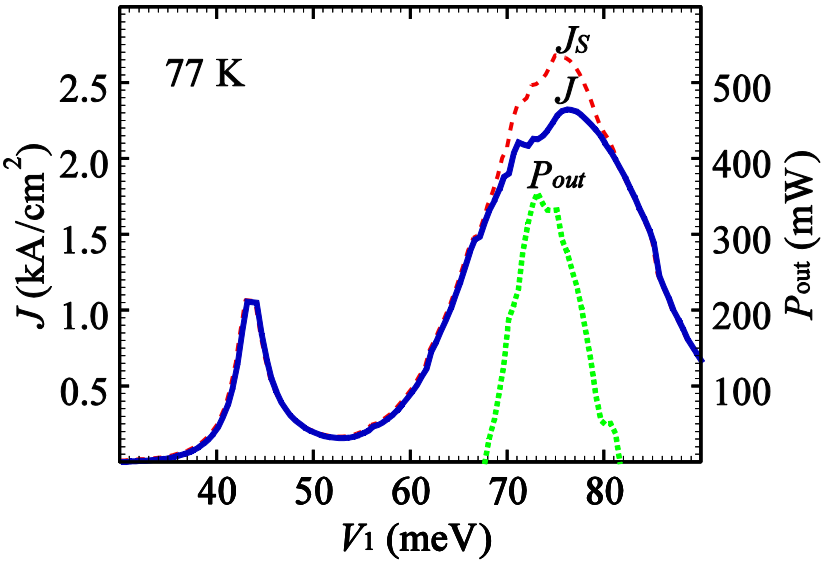

Figure 2. Current-voltage characteristic for the structure with lasing (J_s) and without lasing (J) and power-voltage characteristic.

3. Absorption and gain calculation

In order to estimate the maximum operation temperatures of the given designs, we calculate the dielectric function and cavity losses for a 10 μm thick Au/Ti-Ti/Au waveguide, based on InGaP, as a function of temperature using the method proposed in Ref. [32]. This calculation accounts for the losses in metal layers, on optical phonons and free charge carriers.

The dielectric constant of metals in the THz spectral region is usually described according to the Drude model as

$$\varepsilon_m(\nu) = 1 - \frac{\nu_{pm}^2}{\nu(\nu + i\gamma_{pm})}, \qquad (1)$$

where $\nu_{pm} = (N\, q^2/m_e\, \varepsilon_0)^{1/2}$ is the plasma frequency, N is the free-electron concentration, m_e is the effective electron mass, ε_0 is the vacuum permittivity, and γ_{pm} is the Drude damping parameter. The temperature dependence of the damping parameter was determined through its linear relationship with the temperature dependence of the resistivity of the metal.[32] The values of ν_{pm} and γ_{pm} were calculated to be 9.02 eV and 12.3 meV (80 K) for Au, which agree well with the data of Ref. [32, 33]. We are taking into account absorption in the Ti (5 nm) adhesion layer with parameters ν_{pm}=8.84 eV, γ_{pm}=323.3 meV (80 K).[34, 35] This layer prevents Au diffusion into the epitaxial layers.[2]

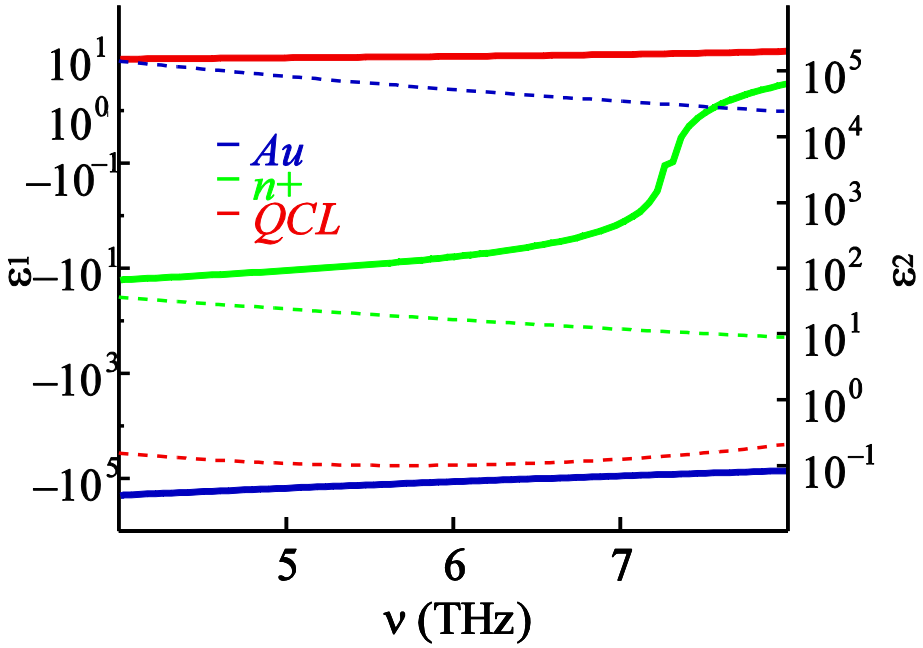

Figure 3. Real ε_1 (solid curves) and imaginary ε_2 (dashed curves) part of the dielectric function spectra for the main components of the QCL waveguide. T = 80 K.

The active region of the QCL is sandwiched between two n^+-InGaP contact layers with a dopant concentration of 10^{18} cm^{-3} (27-nm thick) to form ohmic contacts. The complex dielectric function of semiconductor layers was constructed as a superposition of three damped harmonic oscillators corresponding to the AC- and BC-like phonon modes for ternary alloys $A_{1-x}B_xC$ and to the free carriers, respectively. Hence [36]:

$$\varepsilon(\nu) = \varepsilon_\infty \prod_{j=1}^{N} \frac{\nu^2 - \nu_{LO,j}^2 + i\nu\gamma_{LO,j}}{\nu^2 - \nu_{TO,j}^2 + i\nu\gamma_{TO,j}} - \frac{\nu_{ps}^2}{\nu(\nu + i\gamma_{ps})}, \qquad (2)$$

where ε_∞, $\nu_{LO,j}$, $\nu_{TO,j}$, $\gamma_{LO,j}$, $\gamma_{TO,j}$, ν_{ps}, γ_{ps} represent, in order, the high frequency dielectric constant, the LO-,TO- phonon frequencies and the corresponding phenomenological damping parameters,

semiconductor plasma frequency and the damping parameters of free carriers. The temperature dependence of the damping parameter of semiconductor layers was calculated with the help of the expression: $\gamma_{ps}(T) = q/m_e\mu(T)$, where $\mu(T)$ is the electron mobility as a function of temperature. The dependences of the mobility on temperature and impurity concentration for QCL layers were found on the basis of experimental data using interpolation formulas according to Ref. [37]. The values m_e= 0.0987 free electron mass, μ_{QW}=4207 $cm^2/V{\cdot}s$, μ_{n+}= 800 $cm^2/V{\cdot}s$ common to both $In_{0.49}Ga_{0.51}P$ doped quantum wells and n^+-layers at the 80 K.

The main contribution to losses of the active region and n^+ layers is given by the absorption in $In_{0.49}Ga_{0.51}P$ layers. The highfrequency dielectric function, GaP(1)- and InP(2)-like mode frequencies and dumping parameters (in cm^{-1}) for $In_xGa_{1-x}P$ are approximately given by Ref. [36, 38, 39]:

$$\varepsilon_\infty = 9.11(1-x)+9.61x; \tag{3}$$

$$\begin{aligned}
&\nu_{LO1} = 404.99 - 38.97x - 18.18x^2,\\
&\nu_{TO1} = 395.02 - 54.26x + 6.72x^2,\\
&\gamma_{LO1} = 3.4\frac{T}{300},\ \gamma_{TO1} = 8.1\frac{T}{300}.
\end{aligned} \tag{4}$$

$$\begin{aligned}
&\nu_{LO2} = 394.59 - 80.36x + 30.26x^2,\\
&\nu_{TO2} = 368 - 88.95x + 26.04x^2,\\
&\gamma_{LO2} = 9.5\frac{T}{300},\ \gamma_{TO2} = 9.92\frac{T}{300}.
\end{aligned} \tag{5}$$

In order to obtain the value of dielectric function of the quaternary alloy $(Al_{0.5}Ga_{0.5})_{0.51}In_{0.49}P$ for the barriers we calculated the average of ternary alloys $In_{0.49}Ga_{0.51}P$ and $Al_{0.52}In_{0.48}P$. The high frequency dielectric function, InP(1)- and AlP(2)-like mode frequencies and dumping parameters for $Al_xIn_{1-x}P$ are approximately given by Ref. [36, 40]:

$$\varepsilon_\infty = 7.53x + 9.61(1-x) - 1.72x(1-x); \tag{6}$$

$$\begin{aligned}
&\nu_{LO1} = 350.8x + 344.5(1-x),\\
&\nu_{TO1} = 303.3x + 345.9(1-x),\\
&\gamma_{LO1} = 21\frac{T}{300},\ \gamma_{TO1} = 12.7\frac{T}{300}.
\end{aligned} \tag{7}$$

$$\nu_{LO2} = 501x + 412.4(1-x),$$
$$\nu_{TO2} = 440x + 414.3(1-x), \quad (8)$$
$$\gamma_{LO2} = 5.1\frac{T}{300}, \gamma_{TO2} = 31.3\frac{T}{300}.$$

The dielectric function spectra for the main components of the QCL waveguide is shown in Fig. 3. Calculations of waveguide characteristics were performed for the TM-mode through numerical solution of the wave equation.[32] Calculations of the temperature transformation of the loss and gain spectra are shown in Figure 4 at the value of the applied voltage V_1 = 73 mV. The coefficient of total losses for temperatures 40, 60, 80, 100 K at frequency of 6.7 THz takes values: 55.9, 66.3, 76.6 and 86.7 cm^{-1} respectively. The calculations show contributions to the coefficient from absorption in metal layers, phonon absorption and radiation absorption by free carriers for temperature of 80 K: 19.2, 36.1 and 21.3 cm^{-1} respectively. Reflection losses on the mirrors were taken into account in addition to the waveguide mode losses. For a 1-mm long resonator with reflection coefficient R = 0.55,[41] the reflection losses amounted to 6 cm^{-1}. The maximum of the gain spectrum corresponds to diagonal laser transition *u-l* is realized at 6.7 THz (Fig. 4). The calculations performed for the proposed QCL show that the gain exceeds 100 cm^{-1}, which would allow such a laser to operate up to a sufficiently high temperature of 108 K (Fig. 5). The calculated maximum output power at temperature 77 K is about 350 mW for 100 μm wide and 1 mm long laser cavity (see Fig. 2).

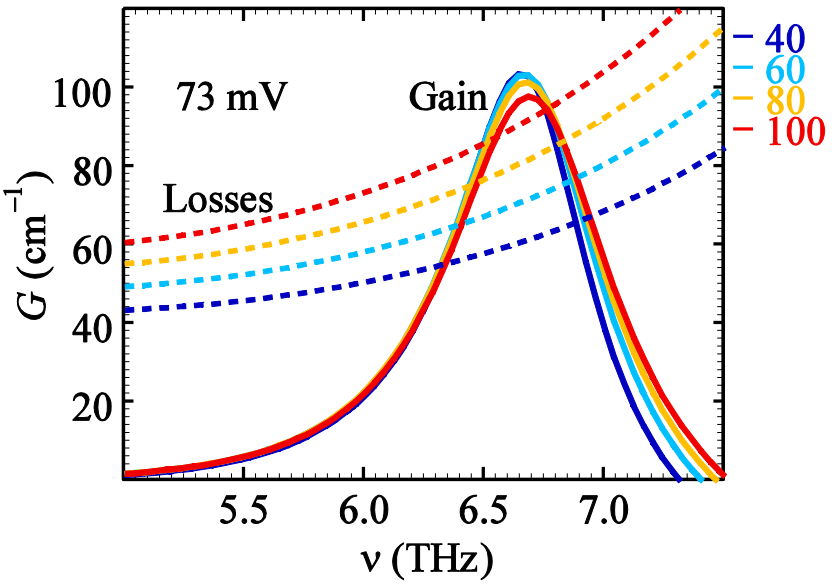

Figure 4. The spectra of gain (solid curves) and the losses (dashed curves) at the value of the applied voltage V_1 = 73 mV for different temperatures.

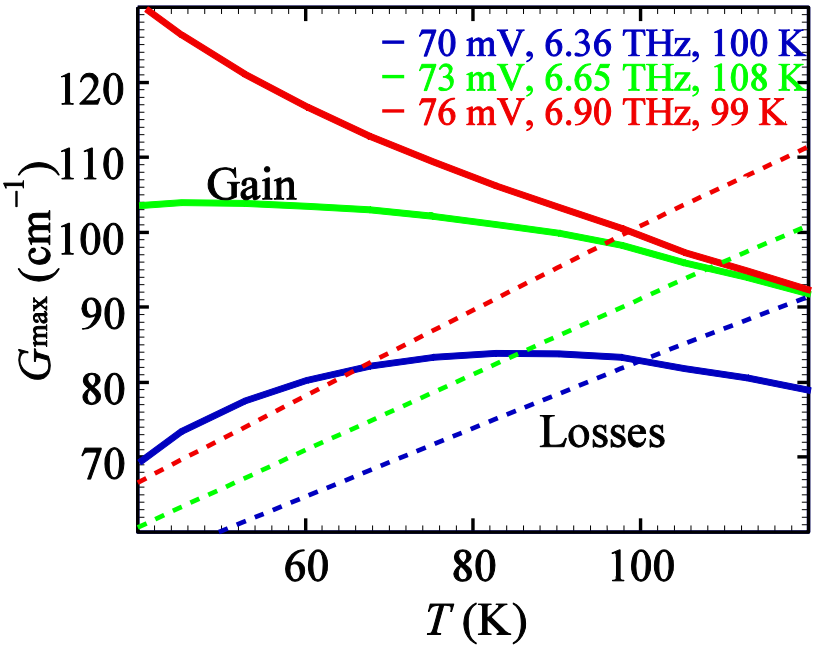

Figure 5. Temperature dependence of the maximum gain (solid curves) and corresponding losses (dashed curves) for different applied voltage per cascade.

4. Conclusion

In conclusion, we summarize the main results of the work. We carried out the modeling of the temperature characteristics of a 6.4-6.9 THz QCL based on GaInP/AlGaInP with a two-QW cascade design and a metal-metal waveguide. The results show the possibility of finding the optimal GaInP/AlGaInP materials and layer thicknesses in order to obtain lasing at temperature up to 100 K. We believe that GaInP/AlGaInP structures can be promising candidates for the QCLs operating in the frequency range of 5.5-7 THz.

Acknowledgements

The work was supported by the Russian Science Foundation, grant # 23-19-00436, https://rscf.ru/project/23-19-00436/.

Received: ((will be filled in by the editorial staff))

Revised: ((will be filled in by the editorial staff))

Published online: ((will be filled in by the editorial staff))

References

[1] R. Kohler, A. Tredicucci, F. Beltram, H. E. Beere, E. H. Linfield, A. G. Davies, D. A. Ritchie, R. C. Iotti, F. Rossi, *Nature* **2002**, *417*, 156-159. DOI: 10.1038/417156a

[2] A. Khalatpour, A. K. Paulsen, C. Deimert, Z. R. Wasilewski, Q. Hu, *Nat. Photon.* **2021**, *15*, 16-20. DOI: 10.1038/s41566-020-00707-5

[3] A. Khalatpour, M. C. Tam, S. J. Addamane, J. Reno, Z. Wasilewski, Q. Hu, *Appl. Phys. Lett.* **2023**, *122*, 161101. DOI: 10.1063/5.0144705

[4] P. D. Cunningham, N. N. Valdes, F. A. Vallejo, et al., *J. Appl. Phys.* **2011**, *109*, 043505. DOI: 10.1063/1.3549120

[5] J. Zhong, T. Mori, T. Kashiwagi, et al., *Spectrochimica Acta Part A: Molecular and Biomolecular Spectroscopy* **2021**, *244*, 118828. DOI: 10.1016/j.saa.2020.118828

[6] R. J. Falconer, A. G. Markelz, *J. Infrared Milli. Terahertz Waves* **2012**, *33*, 973-988. DOI: 10.1007/s10762-012-9915-9

[7] F. M. Al-Douseri, Y. Chen, X.-C. Zhang, *Int. J. Infrared and Millim. Waves* **2006**, *27*, 481-503. DOI: 10.1007/s10762-006-9102-y

[8] M. S. Vitiello, G. Scalari, B. Williams, P. D. Natale, *Opt. Express* **2015**, *23*, 5167-5182. DOI: 10.1364/OE.23.005167

[9] B. Wen, D. Ban, *Prog. Quant. Electron*. **2021**, *80*, 100363. DOI: 10.1016/j.pquantelec.2021.100363

[10] L. Wang, T.-T. Lin, M.-X. Chen, K. Wang, H. Hirayama, *Appl. Phys. Exp*. **2021**, *14*, 112003. DOI: 10.35848/1882-0786/ac2a02

[11] E. Bellotti, K. Driscoll, T. D. Moustakas, and R. Paiella, *J. Appl. Phys.* **2009**, *105*, 113103. DOI: 10.1063/1.3137203

[12] V. P. Sirkeli, O. Yilmazoglu, F. Küppers, and H. L. Hartnagel. *Phys. Status Solidi RRL* **2017**, *11*, 1600423. DOI: 10.1002/pssr.201600423

[13] A. A. Dubinov, D. V. Ushakov, A. A. Afonenko, R. A. Khabibullin, M. A. Fadeev, and S. V. Morozov. *Opt. Lett.* **2022**, *47*, 5048-5051. DOI: 10.1364/OL.470688

[14] A. A. Dubinov, A. Bylinkin, V. Ya. Aleshkin, V. Ryzhii, T. Otsuji, D. Svintsov. *Opt. Express* **2016**, *24*, 29603-29612. DOI: 10.1364/OE.24.029603

[15] W. Terashima and H. Hirayama. *Phys. Status Solidi C* **2011**, *8*, 2302–2304. DOI: 10.1002/pssc.201000878

[16] B. Meng, B. Hinkov, N. M. L. Biavan, H. T. Hoang, D. Lefebvre, M. Hugues, D. Stark, M. Franckie, A. Torres-Pardo, J. Tamayo-Arriola, M. M. Bajo, A. Hierro, G. Strasser, J. Faist, and J. M. Chauveau. *ACS Photonics* **2021**, *8*, 343−349. DOI: 10.1021/acsphotonics.0c01641

[17] D. Yadav, S. Boubanga Tombet, T. Watanabe, S. Arnold, V. Ryzhii and T. Otsuji. *2D Mater*. **2016**, *3*, 045009. DOI: 10.1088/2053-1583/3/4/045009

[18] E. D. Palik. *Handbook of Optical Constants of Solids* (Academic Press, New York, 1985)

[19] O. Madelung. *Semiconductors: Data Handbook* (Springer, New York, 2003).

[20] T. Schwarzback, H. Kahle, M. Jetter, P. Michler, J. Cryst. Growth. **2013**, 370, 208–211. DOI: 10.1016/j.jcrysgro.2012.09.051

[21] Y. Seko, S. Fukatsu, Y. Shiraki, M. Fuse, *J. Appl. Phys*. **1994**, *76*, 1355-1357. DOI: 10.1063/1.357804

[22] S. O'Brien, D. P. Sour, J. R. Shealy, *Appl. Phys. Lett*. **1988**, *53*, 1859-1861. DOI: 10.1063/1.100377

[23] Y. Kaneko, I. Nomura, K. Kishino, A. Kikuchi, *J. Appl. Phys*. **1993**, *74*, 819-824. DOI: 10.1063/1.354872

[24] Y. Kaneko, K. Kishino, *J. Appl. Phys*. **1994**, *76*, 1809-1818. DOI: 10.1063/1.357699

[25] M.-J. Jou, J.-F. Lin, C.-M. Chang, C.-H. Lin, M.-C. Wu, B.-J. Lee, *Jpn. J. Appl. Phys*. **1993**. *32*, 4460-4466. DOI: 10.1143/JJAP.32.4460

[26] K. Yokoyama and K. Hess. *Phys. Rev. B* **1986**, *33*, 5595–5606. DOI: 10.1103/PhysRevB.33.5595

[27] S. M. Goodnick and P. Lugli. *Phys. Rev. B* **1988**, *37*, 2578–2588. DOI: 10.1103/PhysRevB.37.2578

[28] M. Franckié, D. O. Winge, J. Wolf, V. Liverini, E. Dupont, V. Trinité, J. Faist, and A. Wacker. *Opt. Express*, **2015**, *23*, 5201–5212. DOI: 10.1364/OE.23.005201

[29] Y.V. Flores, A. Albo. *IEEE J. of Quantum Electron*., **2017,** *53*, 2300208, DOI: 10.1109/JQE.2017.2689743

[30] D. Ushakov, A. Afonenko, A. Dubinov, V. Gavrilenko, O. Volkov, N. Shchavruk, D. Ponomarev, and R. Khabibullin, *Quantum Electron*. **2019**, *49*, 913–918. DOI: 10.1070/QEL17068

[31] D. Ushakov, A. Afonenko, R. Khabibullin, D. Ponomarev, V. Aleshkin, S. Morozov, and A. Dubinov. *Opt. Express* **2020**, *28*, 25371 – 25382. DOI: 10.1364/OE.398552

[32] D. V. Ushakov, A. A. Afonenko, A. A. Dubinov, V. I. Gavrilenko, I. S. Vasil'evskii, N. V. Shchavruk, D. S. Ponomarev, R. A. Khabibullin, *Quantum Electron*. **2018**, *48*, 1005-1007. DOI: 10.1070/QEL16806

[33] M. A. Ordal, L. L. Long, R. J. Bell, S. E. Bell, R. R. Bell, R. W. Alexander, C. A. Ward, *Appl. Opt*. **1983**, *22*, 1099-1119.

[34] M. A. Ordal, R. J. Bell, R. W. Alexander, L. A. Newquist, M. R. Querry. *Appl. Opt.* **1988**, *27*, 1203-1209.

[35] W. Kemp, P. Klemens, G. White, *Australian J. Phys*. **1956**, *9*, 180-188. DOI: 10.1071/PH560180

[36] T. Hofmann, G. Leibiger, V. Gottschalch, I. Pietzonka, M. Schubert. *Phys. Rev. B* **2001**, *64*, 155206. DOI: 10.1103/PhysRevB.64.155206

[37] V. Palankovski and R. Quay, *Computational Microelectronics* (Springer, New York, 2004).

[38] H. Lee, D. Biswas, M. V. Klein, H. Morkoç, D. E. Aspnes, B. D. Choe, J. Kim, C. O. Griffiths, *J. Appl. Phys*. **1994**, *75*, 5040-5051. DOI: 10.1063/1.355746

[39] R. Ferrini, G. Guizzetti, M. Patrini, A. Parisini, L. Tarricone, B. Valenti, *Eur. Phys. J. B* **2002**, *27*, 449-458. DOI: 10.1140/epjb/e2002-00177-x

[40] H. Asahi, S. Emura, S. Gonda, Y. Kawamura, H. Tanaka, *J. Appl. Phys*. **1989**, *65*, 5007-5011. DOI: 10.1063/1.343173

[41] S. Kohen, B. S. Williams, Q. Hu. *J. Appl. Phys*. **2005**. *97*, 053106. DOI: 10.1063/1.1855394

The GaInP/AlGaInP heterostructures have higher optical phonon energies compared to GaAs/AlGaAs heterostructures. We propose a scheme of phosphides-based terahertz quantum cascade laser. The proposed design has opportunity of operation in a significant part of the GaAs phonon absorption band region, which is inaccessible for existing quantum cascade lasers.

D. V. Ushakov, A. A. Afonenko, R. A. Khabibullin, M. A. Fadeev, and A. A. Dubinov*

Phosphides-based terahertz quantum-cascade laser